THE ANATOMICAL RECORD 298:1237–1254 (2015)

Bone Microstructure of the Stereospondyl *Lydekkerina Huxleyi* Reveals Adaptive Strategies to the Harsh Post Permian-Extinction Environment

AURORE CANOVILLE* AND ANUSUYA CHINSAMY
Department of Biological Sciences, University of Cape Town,
Rhodes Gift 7701, South Africa

ABSTRACT

The small-bodied stereospondyl *Lydekkerina huxleyi*, dominated the amphibian fauna of the South African Lower Triassic. Even though the anatomy of this amphibian has been well described, its growth strategies and lifestyle habits have remained controversial. Previous studies attributed the relative uniformity in skull sizes to a predominance of subadult and adult specimens recovered in the fossil record. Anatomical and taphonomic data suggested that the relatively small body-size of this genus, as compared to its Permo-Triassic relatives, could be linked to a shortened, rapid developmental period as an adaptation to maintain successful breeding populations under harsh environmental conditions. Moreover, *Lydekkerina*'s habitat has been hypothesized to be either aquatic or mainly terrestrial. The current study, utilizes bone microstructure to reassess previous hypotheses pertaining to the biology and ecology of *Lydekkerina*. Various skeletal elements of different-sized specimens are analyzed to understand its growth dynamics, intraskeletal variability, and lifestyle adaptations. Bone histology revealed that our sample comprises individuals at different ontogenetic stages i.e., juveniles to mature individuals. Our results show that these amphibians, despite exhibiting plasticity in growth, experienced an overall faster growth during early ontogeny (thereby attaining sexual maturity sooner), as compared to most other temnospondyls. The microanatomy of the long bones with their thick bone walls and distinctive medullary cavity suggests that *Lydekkerina* may have been amphibious with a tendency to be more terrestrial. Our study concludes that *Lydekkerina* employed a peculiar growth strategy and lifestyle adaptations, which enabled it to endure the harsh, dry conditions of the Early Triassic. Anat Rec, 298:1237–1254, 2015. © 2015 Wiley Periodicals, Inc.

Key words: Triassic; paleohistology; Temnospondyli; habitat; growth pattern; Karoo Basin

The Karoo Basin of Southern Africa is famous for its exceptional Permo-Triassic fossil record in fluvio-lacustrine sediments (Catuneanu et al., 2005; Smith et al., 2012). Although the nonmammalian therapsids have been the subject of intensive studies (e.g., Kemp, 2005; Chinsamy-Turan, 2012; Rubidge, 2013; Kammerer

*Correspondence to: Aurore Canoville, Department of Biological Sciences, University of Cape Town, Private Bag X3, Rhodes Gift, 7701, South Africa. E-mail: canoville.aurore08@gmail.com

Received 12 January 2014; Accepted 19 February 2015.

DOI 10.1002/ar.23160

Published online 23 April 2015 in Wiley Online Library (wileyonlinelibrary.com).

et al., 2014), considerably less attention has been given to basal amphibians, which were abundant members of the Permo-Triassic continental ecosystems (Damiani, 2003; Smith et al., 2012).

Lydekkerina huxleyi is considered to be a basal stereospondyl (Yates and Warren, 2000) that dominated the amphibian fauna (constituting about 74% of the known amphibian fossils) of the Lower Triassic *Lystrosaurus* Assemblage Zone (AZ; Induan–Olenekian) of South Africa (Shishkin et al., 1996; Smith et al., 2012). *Lydekkerina* remains have also been found in coeval deposits of Australia (Warren et al., 2006). Numerous skulls and postcranial material have been uncovered and the anatomy of this amphibian is well described in the literature (Watson, 1920; Broili and Schröder, 1937; Pawley and Warren, 2005; Jeannot et al., 2006; Warren et al., 2006; Hewison, 2007a, 2007b).

Although *Lydekkerina* has been the focus of several anatomical studies, little is known about its growth strategies and lifestyle habits. For instance, the ontogenetic variability of its postcrania is still poorly understood as the size range of most of the described specimens is small (Pawley and Warren, 2004). Although skulls ranging from 49 to 91 mm in length have been described for this taxon (Shishkin et al., 1996; Shishkin and Rubidge, 2000; Hewison, 2007a), majority of them range in lengths between 60 and 80 mm, representing mostly sub-adult and adult individuals according to previous studies (Shishkin et al., 1996; Hewison, 2007a). *Lydekkerina*, as well as some other amphibian genera from the *Lystrosaurus* AZ, such as the rhinesuchid *Broomistega* or the dissorophoid *Micropholis stowi*, constitute small pedomorphic genera with regard to cranial features and body size, in comparison to the larger temnospondyls from the Late Permian and the Middle and Upper Triassic (Shishkin and Rubidge, 2000; Schoch and Rubidge, 2005; Hewison, 2007a). Hewison (2007b) hypothesized that, for *Lydekkerina*, this "dwarfism" could be an adaptation to the difficult and dry climatic conditions that prevailed during the Early Triassic (Smith and Ward, 2001; Pace et al., 2009; Smith et al., 2012), and attributed this feature to the success of these animals after the end Permian extinction event. Hewison (2007a) suggested that the pedomorphism and small body size of this amphibian could be linked to a fast and shortened development, in order to have successful breeding populations. The skull size distribution in the fossil record supports this hypothesis of fast growth and precocious sexual maturity (Hewison, 2007a).

Stereospondyl amphibians have been studied in terms of lifestyle adaptations, but most studies considered predominantly skull features, dentition, postcranial anatomy, and to a lesser extent taphonomy and bone microstructure to infer habitat preferences (e.g., Warren and Snell, 1991; Sanchez et al., 2010; Fortuny et al., 2011; Fernandez et al., 2013). It is traditionally assumed that the evolution of stereospondyls from their Paleozoic temnospondyl ancestors was accompanied by a return to an aquatic lifestyle. Triassic stereospondyls are thus seen as predominantly aquatic or semi-aquatic animals populating freshwater to epicontinental shallow marine environments (Warren and Snell, 1991; Warren, 2000; Steyer, 2002, 2003; Schoch, 2009; Fortuny et al., 2011; Schoch, 2014). Nevertheless, the ecology of small Early Triassic temnospondyls from the *Lystrosaurus* AZ, such as *Lydekkerina huxleyi* (Stereospondyli, Lydekkerinidae), *Micropholis* (Temnospondyli, Amphibamidae) and *Broomistega* (Stereospondyli, Rhinesuchidae) has been debated and they are sometimes described as largely terrestrial and/or fossorial (Hewison, 1996; Shishkin et al., 1996; Shishkin and Rubidge, 2000; Pawley and Warren, 2005). For example, *Lydekkerina* was initially considered to have been aquatic (Shishkin and Rubidge, 2000), but subsequent studies suggested that it was more terrestrial than previously thought (Damiani, 2003; Pawley and Warren, 2005; Jeannot et al., 2006; Hewison, 2007b). The latter assertion was based on the poorly expressed sensory sulci on the skull of *Lydekkerina*, as well as its well-ossified long bone epiphyses, autopod elements, and postcranial skeleton in general, as compared to other Triassic stereospondyls. Hewison (2007b) also suggested a sporadic fossorial lifestyle for estivation to escape seasonal drought.

Previous paleobiological inferences for *Lydekkerina* were almost exclusively drawn from anatomical and taphonomic studies. However, long bone histological examination allows a direct assessment of various aspects of tetrapod paleobiology, such as ontogeny, growth patterns, and lifestyle (Chinsamy-Turan, 2005; Ricqlès, 2011; Chinsamy-Turan, 2012; Padian and Lamm, 2013). Long bone and osteoderm histology has been examined in ecologically diverse temnospondyls from the Permian and Triassic (Damiani, 2000; Steyer et al., 2004; Mukherjee et al., 2010; Sanchez et al., 2010; Witzmann and Soler-Gijón, 2010; McHugh, 2012; Konietzko-Meier and Klein, 2013; Konietzko-Meier and Sander, 2013; Konietzko-Meier and Schmitt, 2013; Sanchez and Schoch, 2013; McHugh, 2014), but only one recent study included a humerus of *Lydekkerina* (McHugh, 2012). In the present study, we apply histological and microanatomical approaches to reassess previous hypotheses pertaining to the biology and ecology of *Lydekkerina*. The bone microstructure of various skeletal elements of different-sized specimens is analyzed to understand its growth strategies, intraskeletal variability and lifestyle adaptations.

MATERIAL AND METHODS

Biological Sample

All the specimens sampled in this study pertain to the monospecific genus *Lydekkerina huxleyi*, and were recovered from the *Lystrosaurus* AZ of South Africa, corresponding to the Lower Triassic (Table 1). These specimens are curated in various South African museum collections [institutional abbreviations: BP/I/, Evolutionary Studies Institute (previously Bernard Price Institute), Witwatersrand University, Johannesburg; TM, Ditsong National Museum of Natural History, Pretoria (previous Transvaal Museum); NMQR, Karoo Paleontology, National Museum, Bloemfontein].

To document growth patterns, and inter-bone histovariability, we examined 15 skeletal elements (humerus, radius, ulna, femur, rib) of different sized specimens (Table 1; Fig. 1). Limb bones were preferentially used as they exhibit the least secondary remodeling in the midshaft region as compared to other skeletal elements, therefore providing the best record of the primary bone tissue (Francillion-Vieillot et al., 1990). Femora were the most persistent skeletal elements available for

TABLE 1. Material of *Lydekkerina* sampled for histological assessment

Specimen number	Description	Skull median length (mm)	Skeletal element	Bone maximal length (mm)	Section type
BP/I/5021	Block containing the back of a skull associated with postcranial elements	49 – 54.4[a]	Femur	18.7	CS diaphysis CS metaphysis (X2) LS distal epiphysis
BP/I/5022	Skull and postcranial elements	59.6	Humerus	24.5	CS diaphysis CS metaphysis
			Rib fragment	–	CS
NMQR 665	Skull and postcranial elements	64.4	Radius	13.0	CS diaphysis (X2) CS metaphysis CS epiphysis
			Ulna	14.6	CS diaphysis (X2) CS metaphysis CS epiphysis
			Rib fragment	–	CS
			Unidentified bone	–	CS
TM 186	Partially prepared block with six skulls and some postcranial material (all the specimens seems to be at the same ontogenetic stage)	62–67[b]	Femur 1	20.0[b]	CS diaphysis CS metaphysis
			Femur 2	19.9[b]	CS diaphysis (X3) CS metaphysis
			Femur 3	19.6[b]	CS diaphysis (X2) CS metaphysis
			Unidentified long bone	–	CS diaphysis
TM 85	Skull and pectoral girdle (described in Pawley and Warren, 2005)	73.3	Radius	15.9	CS diaphysis CS metaphysis
			Rib fragment	–	CS
BP/I/1373	Partially prepared block with three skulls and postcranial material (described in Pawley and Warren, 2005)	79.5–82.1	Femur	30.8	CS diaphysis (X3) CS metaphysis LS epiphysis
			Rib	–	CS

See the Material and Methods section for institutional abbreviations. Abbreviations: CS, cross-section; LS, longitudinal section.
[a]Skull length approximated from skull width and skull dimensions for *Lydekkerina* recorded in the literature (Shishkin et al., 1996; Shishkin and Rubidge, 2000).
[b]These measurements are approximate since the skeletal elements were not complete or were still partially embedded in the sediment.

histological examination (five femora ranging from 18.7 to 30.8 mm in length).

Most of the postcranial elements sampled were directly associated with skulls (Table 1, see also Fig. 1). Almost the complete range of skull sizes known for *Lydekkerina* in the fossil record is represented in our sample (see Shishkin et al., 1996; Hewison, 2007a; Fig. 1A).

The following section provides a brief description of the specimens sampled for this study (Table 1).

BP/I/5021. This specimen consists of the back of a skull associated with some postcranial elements (some vertebrae, ribs, an almost complete femur; Fig. 1B). The width of the skull has been compared to skull measurements documented in the literature for *Lydekkerina* (Shishkin et al., 1996; Shishkin and Rubidge, 2000), and its midline length has been estimated to be about 49–54.4 mm. According to Shishkin et al., (1996) and Shishkin and Rubidge (2000), this individual represents a juvenile. The femur of this specimen was sampled for histological analysis.

BP/I/5022. This specimen represents a skull (59.6 mm in midline length) associated with semiprepared postcranial material. A humerus and a rib were sampled for histological analysis.

NMQR 665. This specimen comprises a skull (64.4 mm in midline length) and some disarticulated postcranial elements. We sampled the associated radius and ulna (still in articulation) and a rib fragment for histological analysis.

TM 186. This specimen consists of six partial skulls associated with disarticulated postcranial elements. Histological sections were prepared from three femora and an unidentified long bone (Fig. 1C). It was not possible to associate the limb bones to the different skulls. However, several factors suggest that the sampled femora indeed belong to the skulls. First of all, the skulls have similar sizes (from 62 to 67 mm in midline length) and probably represent amphibians of the same age cohort, as often seen in other accumulations of *Lydekkerina* specimens (see Pawley and Warren, 2005; Hewison, 2007a). This observation also applies to the three sampled femora, which have comparable lengths (Table 1). The size of these femora matches the size of the associated skulls, considering previous descriptions of *Lydekkerina*. Second, some limb bones are still in articulation,

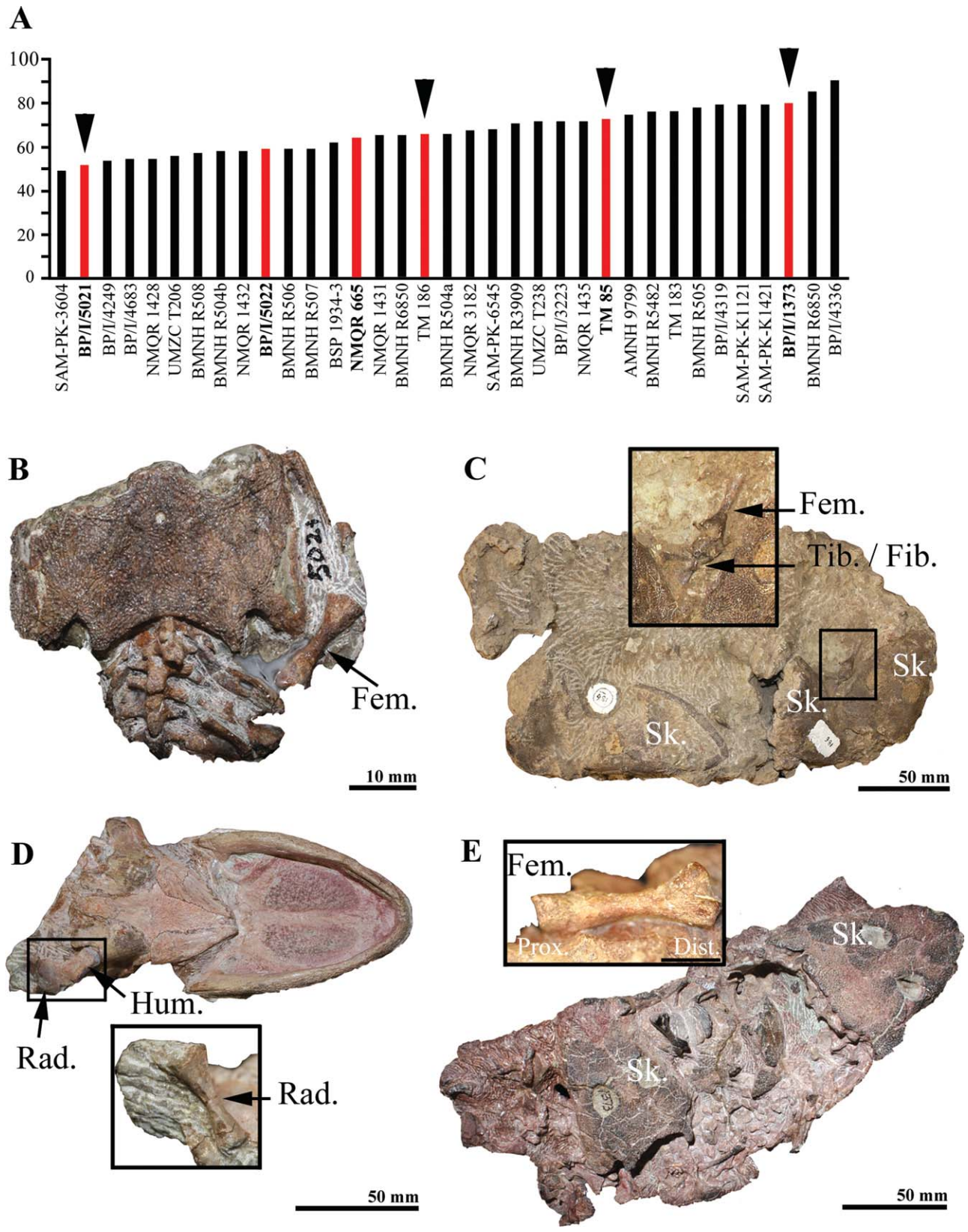
A
100
80
60
40
20
0
SAM-PK-3604
BP/I/5021
BP/I/4249
BP/I/4683
NMQR 1428
UMZC T206
BMNH R508
BMNH R504b
NMQR 1432
BP/I/5022
BMNH R506
BMNH R507
BSP 1934-3
NMQR 665
NMQR 1431
BMNH R6850
TM 186
BMNH R504a
NMQR 3182
SAM-PK-6545
BMNH R3909
UMZC T238
BP/I/3223
NMQR 1435
TM 85
AMNH 9799
BMNH R5482
TM 183
BMNH R505
BP/I/4319
SAM-PK-K1121
SAM-PK-K1421
BP/I/1373
BMNH R6850
BP/I/4336
B
Fem.
10 mm
C
Fem.
Tib. / Fib.
Sk.
Sk.
Sk.
50 mm
D
Hum.
Rad.
Rad.
50 mm
E
Fem.
Prox.
Dist.
Sk.
Sk.
50 mm

Fig. 1.

indicating that there was only some dispersal of the carcasses before burial (see Fig. 1C).

TM 85. This specimen represents a skull in articulation with the pectoral girdle (skull midline length, 73.3 mm; described in Pawley and Warren, 2005). A radius as well as a rib fragment was sampled for histological analysis (Fig. 1D).

BP/I/1373. This specimen constitutes a partially prepared block with three large skulls (midline lengths from 79.5 to 82.1 mm) and associated postcranial material (Fig. 1E) (Pawley and Warren, 2005). These animals are the largest individuals of our sample. Pawley and Warren (2005) described these specimens as mature adults at the time of death. We sampled a femur and a piece of a rib from this block.

Thin-Section Preparation and Histological Descriptions

All specimens were photographed before sampling and standard-measurements of skull and long bone length were recorded (Table 1). The bones were sampled using a small Dremel® diamond saw and care was taken to minimize damage to the specimens. Samples were then embedded in a polyester resin, cut with a diamond saw, and finally polished to desired thickness following the protocol of Chinsamy and Raath (1992). The histological descriptions follow those of Francillion-Vieillot et al. (1990) and Chinsamy-Turan (2005, 2012).

Each bone was studied at the microanatomical and histological level. Where possible, several sections have been made of a given skeletal element; i.e., transverse sections at the diaphyseal and metaphyseal levels, and longitudinal sections of the epiphyses (Fig. 2A).

Measurements were taken on the cross-sections in order to assess the thickness of the bone walls, the relative size of the medullary region, as well as the overall compactness of the section (Fig. 2B, Table 2). The cortical thickness index, or *k* index (Currey and Alexander, 1985) was calculated as the ratio of the medullary cavity diameter (MCd) divided by the section diameter [(CSw+CSl)/2]. The *k* index varies between 0 and 1, where lower values are associated with thicker bone walls, and higher values correspond to thinner bone walls. The cortical thickness parameter (RBT%) was also calculated for some sections, as the ratio of the average bone wall thickness to the average cross-sectional diameter and expressed as a percentage of the diameter (Mukherjee et al., 2010). These parameters, often used in comparative osteology, give a biased estimate of the bone compactness, because they do not take into account the vascular canals and resorption cavities. Nevertheless, it allows a comparison with previous studies that used such cortical thickness indices (e.g., Currey and Alexander, 1985; Castanet and Caetano, 1995; Botha and Chinsamy, 2004; Botha-Brink and Angielczyk, 2010; Botha-Brink and Smith, 2012). When the preservation was good enough, we also measured bone compactness (Comp.) with Bone Profiler (Girondot and Laurin, 2003), a program that allows for a precise evaluation of bone compactness with the inclusion of vascularization and resorption spaces (Table 2). Moreover, bone profiler allows extracting compactness profile parameters of a sigmoid mathematical model, which shows the distribution of the bony tissue in a section. Several lifestyle inference models have been built from these compactness profile parameters and applied to fossil taxa (e.g., Canoville and Laurin, 2010; Quemeneur et al., 2013). We applied the models developed by Germain and Laurin (2005) (but available in Laurin et al., 2011) and Quemeneur et al. (2013) based respectively on the microanatomy of the radius and the femur of amniotes to some of the sampled long bones. Finally, at the adult stage, the femur of *Lydekkerina* has a prominent adductor crest on its ventral side (Pawley and Warren, 2005; Hewison, 2007b). Where possible, the development of this crest was expressed as a ratio between the greatest length (given through the adductor crest on the dorsoventral axis, CSl) and the width of the femoral cross section (CSw), in order to provide additional information to infer the ontogenetic stage of the studied specimens (Fig. 2B).

RESULTS

Bone Microstructural Descriptions

Bone microanatomical and histological descriptions of *Lydekkerina* material are listed from the smallest skull-sized specimens to the largest ones. For some specimens, the bone histology was poorly preserved, thereby limiting the consequent descriptions. The main microstructural features for this stereospondyl amphibian are then summarized considering variation among individuals and interskeletal element variability.

Fig. 1. (**A**) Skull size range (midline length in mm) for representative *Lydekkerina huxleyi* specimens found in the fossil record. Data were gathered from Shishkin et al., (1996), Hewison (2007a), and the present work. The specimens sampled in our study are highlighted in red and are well distributed within the skull-size range known for *Lydekkerina* (49–91 mm). The specimens marked by an arrow are presented in B–E. (**B**) Specimen BP/I/5021 represents the back of a skull in dorsal view (estimated midline length of 49–54.4 mm) associated with some postcranial elements. The femur was sampled for histological analysis (length = 18.7 mm). (**C**) Specimen TM 186 is a semi-prepared block with six partial skulls (with an average midline length of 65.7 mm) associated with some disarticulated or partially articulated postcranial elements. The close-up shows one of the three femora that have been sectioned (about 20 mm in length). (**D**) Specimen TM 85 represents a skull (midline length of 73.3 mm, ventral view) in connection with the pectoral girdle. The close-up shows the sectioned radius (length = 15.9 mm) preserved in articulation with the left humerus. (**E**) Specimen BP/I/1373 constitutes a partially prepared block with three large skulls (skull sizes range from 79.5 to 82.1 mm) and semiarticulated postcranial material. These individuals represent the largest specimens of our sample. We sampled a femur presented in dorsal view in the close-up (length = 30.8 mm). Abbreviations: BP/I/, Evolutionary Studies Institute (previously Bernard Price Institute), Witwatersrand University, Johannesburg; TM, Ditsong National Museum of Natural History, Pretoria (previous Transvaal Museum); SAM-PK, Iziko South African Museum, Cape Town; NMQR, Karoo Palaeontology, National Museum, Bloemfontein; BMNH, Natural History Museum, London, UK; UMZC, University Museum of Zoology, Cambridge, UK; Dist., distal; Fem., femur; Fib., fibula; Hum., humerus; Prox., proximal; Rad., radius; Sk., skull; Tib., tibia.

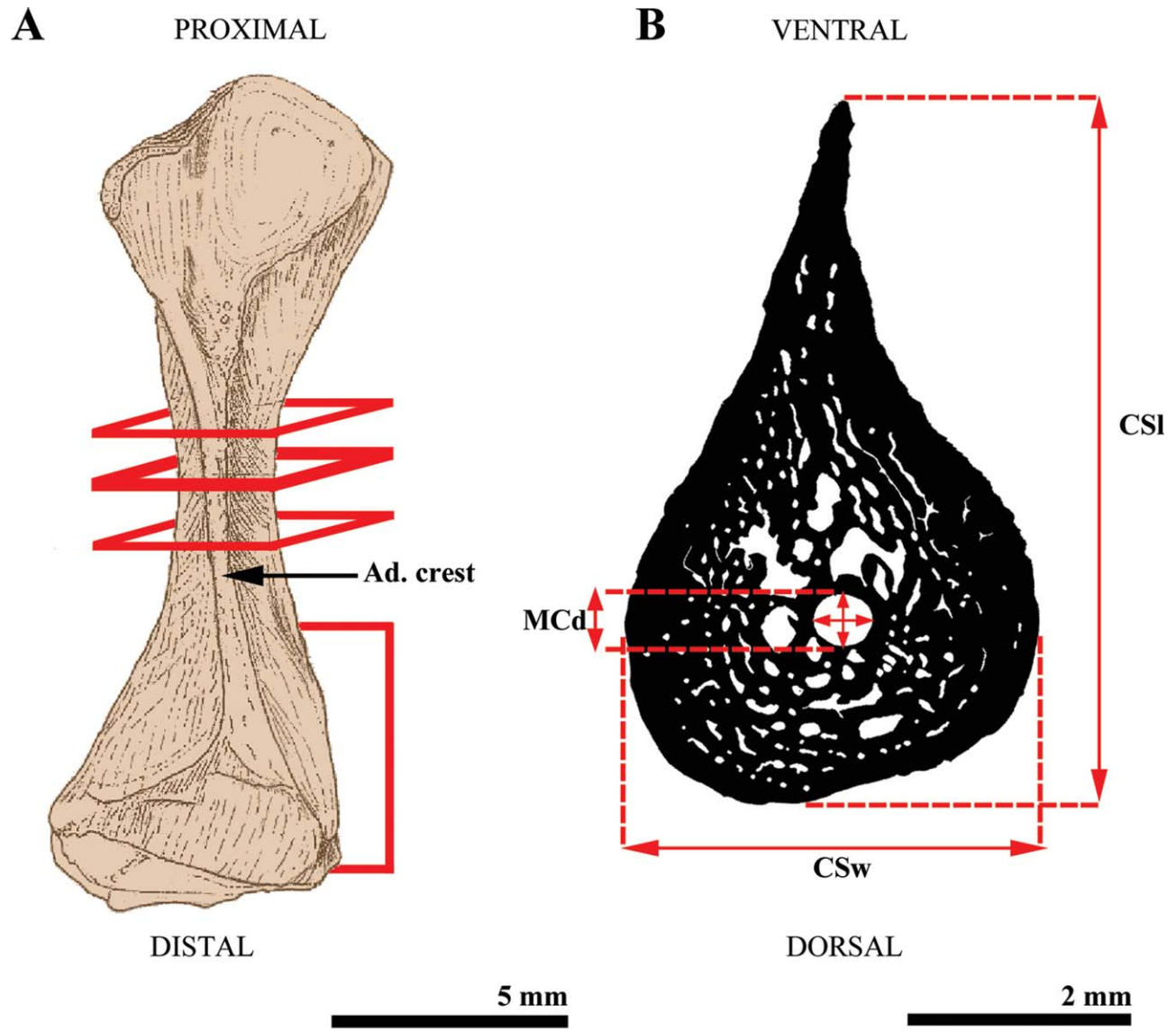

Fig. 2. Measurements taken on the long bones sampled and the cross-sections. **(A)** Ventral view of a femur of an adult specimen of *Lydekkerina huxleyi* (modified from Hewison, 2007b). Prior to sectioning, the long bones were photographed and their maximal lengths were recorded. The thick red lines represent the different section planes; i.e. mid-diaphyseal, metaphyseal transverse sections, and epiphyseal longitudinal section. **(B)** Drawing of the mid-diaphyseal cross-section (l) of the sampled femur of specimen BP/I/1373. For each bone, measurements were taken (see Table 2) to quantify the size of the medullary cavity proportionally to the bone wall thickness as detailed in the Material and Methods section. The development of the adductor crest was measured on the femora. Abbreviations: Ad. crest, adductor crest; MCd, medullary cavity diameter; CSw, cross-section width; CSl, cross-section length.

BP/I/5021. To assess intraelement histovariability, the femur of this specimen was cut in three different regions (cross-section close to the mid-diaphysis, Fig. 3A; metaphysis, Fig. 3B; longitudinal section of the distal epiphysis, Fig. 3C). At the diaphyseal level, the medullary cavity is sub-circular, and well delimited by an inner circumferential layer consisting of endosteally formed lamellar bone (ICL) with flatten osteocyte lacunae (Fig. 3D). Few slender trabeculae are visible in the medullary region. The bone wall is moderately thick (k index of 0.29, RBT of 35.1%; Table 2) but has a porous aspect because of the high number of large open spaces of the incipient primary osteons and simple vascular canals (compactness of 0.70). Resorption cavities are present in the perimedullary region and preferentially located on the ventral side of the section, at the base of the adductor crest. The cortex is stratified into two regions corresponding to two growth cycles, highlighted in polarized light (Fig. 3D). The first growth cycle comprises a narrow zone of parallel fibered bone in the deep cortex, followed by a thin annulus of parallel fibered to lamellar bone (Fig. 3D). The second growth cycle is formed of a well-vascularized bone tissue formed of a poorly organized parallel-fibered matrix with plump osteocyte lacunae. The adductor crest is moderately developed on the ventral side of the diaphyseal cross-

TABLE 2. Measurements of some skeletal element cross-sections (taken as shown on Fig. 2B)

Specimen	Bone	Bone length (mm)	CS level	MCd (mm)	CSw (mm)	CSl (mm)	Ratio CSl/CSw	k index	RBT %	Comp.
BP/I/5021	Femur	18.7	Diaphysis	0.82	2.24	3.44	1.54	0.29	35.1	0.70
			Metaphysis	1.22	2.26	3.62	1.59	0.41	22.8	–
BP/I/5022	Humerus	24.5	Diaphysis	0.64	3.25	4.72	–	0.16	40.9	–
NMQR 665	Radius	13.0	Diaphysis 1	0.50	1.55	2.03	–	0.28	35.1	0.83
			Diaphysis 2	0.55	1.55	2.08	–	0.30	–	–
			Metaphysis	–	2.39	2.95	–	–	–	–
	Ulna	14.6	Diaphysis 1	0.89	1.63	2.05	–	0.48	26.6	0.71
			Diaphysis 2	0.80	1.55	1.88	–	0.47	–	–
			Metaphysis	–	3.44	5.23	–	–	–	–
TM 186	Femur 1	20.0	Diaphysis 1	0.77	3.02	–	–	–	–	0.45
	Femur 2	19.9	Diaphysis 1	0.68	3.40	4.40	1.29	0.17	–	–
			Diaphysis 2	0.74	3.23	4.06	1.26	0.20	39.4	–
			Diaphysis 3	0.91	3.14	4.08	1.30	0.25	–	–
	Femur 3	19.6	Diaphysis 1	0.57	2.18	2.95	1.35	0.22	39.0	0.68
			Diaphysis 2	0.83	2.43	2.88	1.19	0.31	–	–
TM 85	Radius	15.9	Diaphysis	0.49	1.49	1.99	–	0.28	35.9	0.85
			Metaphysis	1.26	1.95	2.33	–	0.59	–	–
BP/I/1373	Femur	30.8	Diaphysis 1	0.49	3.72	6.21	1.67	0.10	44.8	0.85
			Diaphysis 2	0.81	3.67	6.38	1.74	0.16	41.7	0.79
			Diaphysis 3	1.10	3.69	6.59	1.79	0.21	39.4	–
			Metaphysis	1.72	4.08	7.04	1.73	0.31	–	–

Abbreviations: Comp., compactness calculated in Bone Profiler (Girondot and Laurin, 2003); CS, cross-section; CSl, maximal cross-section length (along the dorso-ventral axis for the femur); CSw, cross-section width (perpendicular to CSl); MCd, medullary cavity diameter. For the femur, the ratio CSl/CSw gives an estimate of the development of the adductor crest. A ratio close to 1 would indicate that the adductor crest is not developed. Higher is the ratio, more developed is the adductor crest; k index (Currey and Alexander, 1985) is calculated as a ratio between the medullary cavity diameter (MCd) and the section diameter [(CSw + CSl)/2]. The cortical thickness parameter (RBT%) was also calculated for some sections. Note that some of these measurements are approximations because of the poor preservation of some sections.

section (Table 2). In this area, the vascular canals tend to run parallel to the crest axis and the bone matrix is parallel-fibered to lamellar. The bone microstructure is similar at the metaphyseal level (Fig. 3B,E), even though the medullary region is enlarged and filled by a loose mesh of thin bone trabeculae (Table 2). The bone surface is uneven and pierced by vascular canals (Fig. 3A,B,E). In the epiphysis, the bone histology is not well preserved (Fig. 3C,F). The distal epiphysis has a pitted surface probably because of incomplete ossification. The bone wall at this level is thin and becomes thinner (160 – 440 μm) towards the articular surface. Some trabeculae (25–40 μm thick) form a loose mesh in the medullary region (Fig. 3C,F). All these microstructural features, such as a well-vascularized parallel-fibered bone tissue in the cortex, an uneven bone surface and poorly ossified epiphyses, are characteristic of a juvenile individual and suggest that this animal was still actively growing at the time of death.

BP/I/5022. The bone histology of the humerus at both diaphyseal (CSl = 4.72 mm) and metaphyseal (CSl = 6.88 mm) levels is well preserved even though the sections are incomplete (Fig. 3G,H). At the mid-diaphyseal level (Fig. 3G), the cross-section reveals several large cavities in the central part of the bone. However, one large cavity, close to the center of the cross-section, with a regular sub-circular shape, is well delimited by an ICL consisting of a lamellar endosteal bone and is most probably the medullary cavity (Fig. 3G). Although the bone wall is thick (k index of 0.16, RBT of 40.9%; Table 2), the overall compactness is low because of several large irregular erosion spaces in the deep cortex. One cavity is almost as wide as the presumed medullary cavity and is bordered by an irregular layer of endosteal lamellar bone (Fig. 3G). At the metaphyseal level, the medullary region is wider and occupied by an endosteal spongiosa (Fig. 3H). In both sections, different bone tissues are observed in the cortex. Despite extensive resorption and secondary reconstruction, patches of a woven bone matrix are visible in the deep cortex (Fig. 3I,J). The vascularization decreases toward the periphery and the bone matrix becomes parallel-fibered (Fig. 3I,J). A layer of avascular lamellar bone with closely spaced rest lines is visible in some parts of the outermost cortex (Fig. 3J) and attests to a significant slowdown in growth at the time of death. Where preserved, the bone surface is smooth and even. In a restricted area of both sections, the bone tissue is mostly parallel fibered, and numerous plumb osteocyte lacunae associated with long Sharpey's fibers exhibit a radial orientation, suggesting a zone of muscle or tendon insertion (Fig. 3K). The rib cross-section is incomplete (CSl = 2.72 mm; Fig. 3L). The medullary region is large, well defined and occupied by a loose network of bone trabeculae (Fig. 3L, M). The bone wall is thin. The deep cortex is formed by a thin layer of poorly vascularized woven bone matrix with few primary and secondary osteons (Fig. 3M). In polarized light, bundles of Sharpey's fibers are visible in the cortex. Toward the periphery, the bone matrix consists of an avascular lamellar bone interrupted by closely spaced rest lines (Fig. 3M). The microstructure of both bones is congruent and

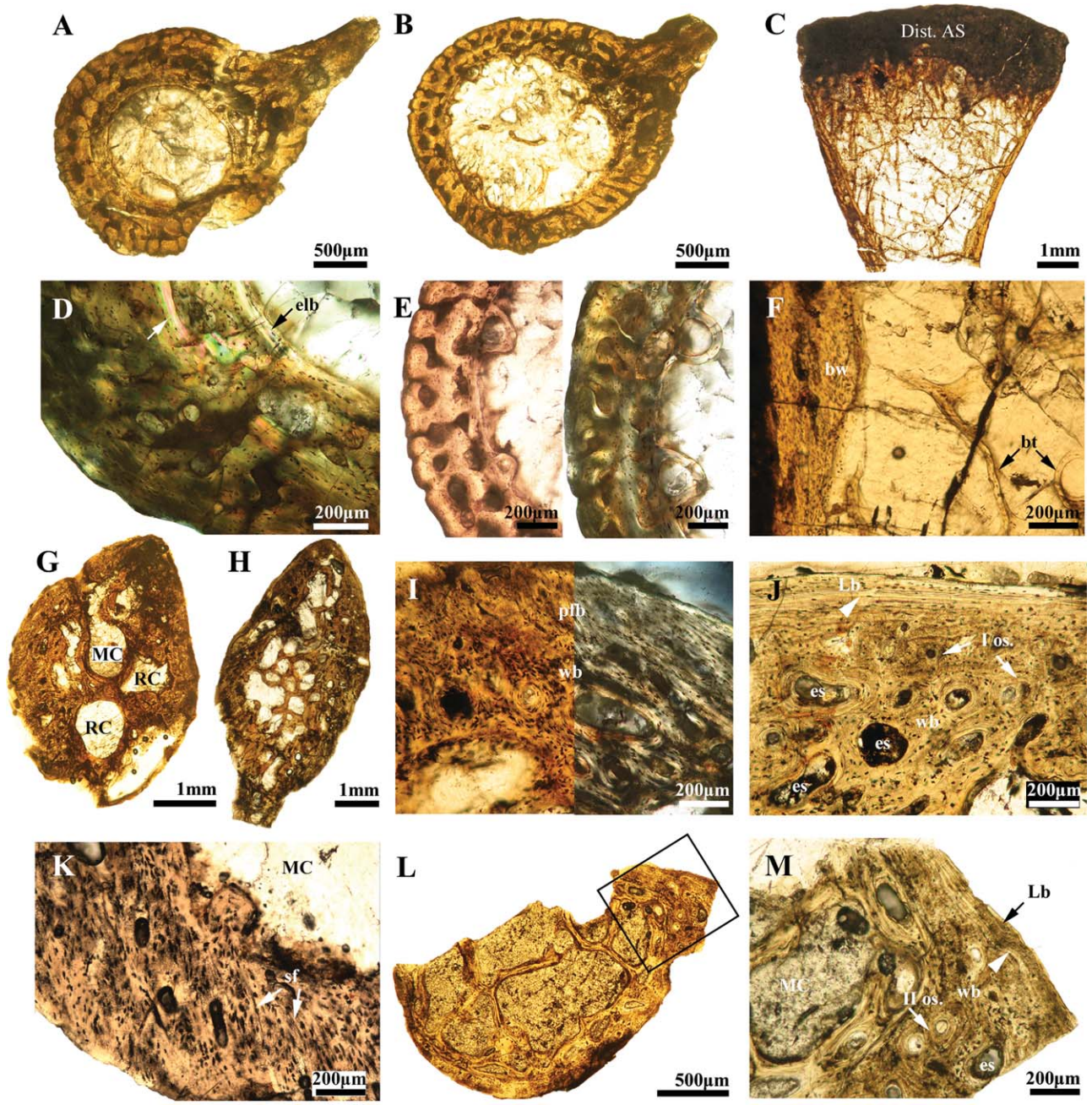

Fig. 3. Bone microstructure of the small specimens BP/I/5021 (A–F) and BP/I/5022 (G-M) of *Lydekkerina* sampled in the present study. (**A)** Diaphyseal cross-section of a femur. (**B)** Cross-section of the proximal metaphysis of the femur. (**C)** Longitudinal section of the distal epiphysis of the femur. Note the thin bone walls and the medullary region infilled by a loose mesh of thin bony trabeculae. The articular surface is not well ossified and has been infilled with sediment. (**D)** Higher magnification of the femoral cortex in A in polarized light. Note the growth mark (white arrow) represented by a thin annulus of lamellar bone. (**E)** Higher magnifications of the femoral bone wall in B in normal (left) and polarized (right) light. The bone surface is uneven and numerous vascular canals pierce the surface. (**F)** Higher magnification of the epiphyseal microstructure in C. (**G)** Mid-diaphyseal cross-section of the humerus. (**H)** Metaphyseal cross-section of the humerus. (**I)** Higher magnification of the cortex in G in normal (left) and polarized (right) light. (**J)** Higher magnification of the cortex in H. The inner cortex is formed of a woven bone matrix with primary osteons. Large erosion spaces with centripetal deposits of lamellar bone are present in the deep cortex. The vascularization decreases towards the periphery and the bone matrix gets more organized. In this region of the bone, a layer of avascular lamellar bone with closely spaced rest lines (arrow head) is visible in the outer cortex. (**K)** Higher magnification of the cortex in H. Note the density and orientation of the osteocyte lacunae, as well as Sharpey's fibers suggesting a zone of muscle attachment. (**L)** Incomplete cross-section of a rib. (**M)** Higher magnification of the bone wall in L. A layer of avascular lamellar bone with rest lines (arrow head) is visible in the outermost cortex. Abbreviations: bt, bone trabeculae; bw, bone wall; Dist. AS, distal articular surface; elb, endosteal lamellar bone; es, erosion space; Lb, lamellar bone; MC, medullary cavity; I os., primary osteon; pfb, parallel-fibered bone; RC, resorption cavity; sf, Sharpey's fibers; wb, woven bone.

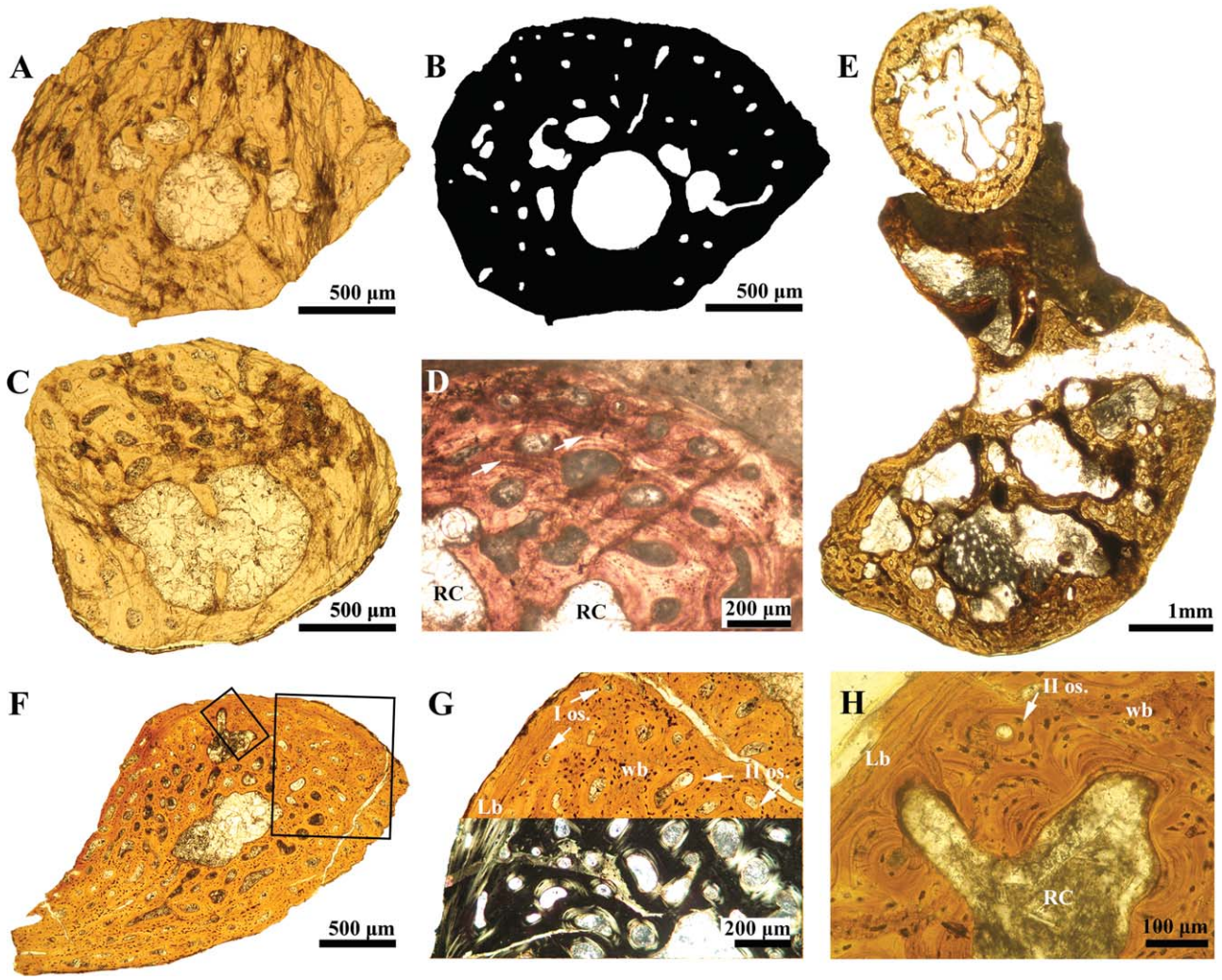

Fig. 4. Bone microstructure of specimen NMQR 665. (**A**) Mid-diaphyseal cross-section of a radius. (**B**) Interpretative drawing of the section in **A** highlighting the vascular canals and the resorption cavities. (**C**) Mid-diaphyseal cross-section of the associated ulna. (**D**) Outer half of the cortex of the radius in a section close to the diaphyseal level. Large resorption cavities are present in the deep cortex. At least two thin annuli of lamellar bone (arrows) are visible and alternate with well-vascularized zones. (**E**) Cross-sections of the radius (top) and ulna (bottom) close to the epiphysis. (**F**) Cross-section of a rib. (**G**) Higher magnification of the bone wall of the rib in **F** in normal (top) and polarized light (bottom). Most of the cortex is formed of a fibrolamellar bone tissue. Numerous erosion spaces with centripetally deposited lamellar bone are visible in the deep cortex. A layer of avascular lamellar bone is visible in the outermost cortex of the rib. (**H**) Higher magnification of the bone wall of the rib in **F**. Note the large resorption cavity and the plump osteocyte lacunae in the interstitial woven bone. Abbreviations: I os., primary osteon; II os., secondary osteon; Lb, lamellar bone; RC, resorption cavity; wb, woven bone.

suggests that after a phase of fast growth early in ontogeny, the growth slowed down drastically. This individual was thus mature at the time of death.

NMQR 665. Both the radius and the ulna have been sampled in cross-sections at the mid-diaphyseal level (Fig. 4A–C), in the shaft, but closer to the metaphysis (Fig. 4D), as well as close to the epiphysis (Fig. 4E). The microstructure of these bones is similar, but their histology is poorly preserved due to numerous cracks and the loss of the optical properties of the bone matrix when observed in polarized light. At the mid-diaphyseal level (Fig. 4A–C), the bone wall is thick and compact (compactness in the radius and the ulna equals 0.83 and 0.71, respectively, see also Table 2). The medullary cavity is well defined, free of bone trabeculae and small (especially in the radius with a k index of 0.28, RBT of 35.1%; Table 2). In both skeletal elements, a thick ICL consisting of endosteally formed lamellar bone surrounds the medullary cavity. Vascular canals are sparse (Fig. 4A–C) and consist of large primary and secondary osteons. Small erosion spaces with deposition of circumferential lamellar bone as well as few larger resorption cavities can be observed in the deep cortex of both elements. Some islands of cortical bone preserved their optical properties and testify that the deep primary bone was woven to parallel fibered (isotropic to slightly anisotropic bone matrix). At least two thin annuli of lamellar bone are visible in the outer half of the cortex

in both elements (Fig. 4D) attesting of a periodic slow down of the growth. The bone surface is smooth where the outer layer of the cortex is preserved. Close to the epiphyseal level, the bone microanatomy of the radius is different from that of the ulna (Fig. 4E). The bone wall of the radius is thin (330–209 μm) and the medullary region very large with few, thin trabeculae. The section of the ulna is much larger than the section of the radius. The bone wall is also thin, but the medullary region is not well defined and infilled by thick bone trabeculae. The cortex is formed by a well-vascularized woven or parallel fibered matrix, depending on the region of the bone, with numerous and plumb osteocyte lacunae.

The section of the rib has a porous aspect because of the high degree of vascularization and the presence of enlarged cavities in the deep cortex (Fig. 4F–H). The bone wall is thick and limits the extent of the medullary cavity, which is well defined and free of bone trabeculae. Secondary reconstruction is important in the deep cortex, but islands of primary bone attest of a woven bone matrix (Fig. 4G,H). The osteocyte lacunae are numerous, disorganized and globular (Fig. 4G,H). The vascular canals have a preferential longitudinal orientation and are mostly primary and secondary osteons (Fig. 4G,H). In some regions of the outermost cortex, a layer of avascular parallel-fibered to lamellar bone is visible (Fig. 4G,H). Finally, the unidentified long bone has a small and round cross-section (CSl = 1.08 mm). The bone wall is thick and the medullary cavity is reduced, but free of bony trabeculae. The cortex presents few vascular canals.

TM 186. The three femora sampled exhibit similar bone microstructure. The diaphyseal cross-section of Femur 1 (Fig. 5A; Table 1) is incomplete and preserves only the dorsal side (thus, the development of the adductor crest is not observed). For Femur 2 (Fig. 5B,C) and 3 (Fig. 5G), the adductor crest is moderately developed as compared to the largest specimen BP/I/1373 (Table 2). For each femur, the medullary cavity is relatively small at the mid-diaphyseal level (Table 2), well defined, circular and bordered by a thin ICL consisting of a layer of endosteally formed lamellar bone (Fig. 5H). The bone wall is thick but numerous vascular canals, as well as large resorption cavities in the deep cortex (and especially at the base of the adductor crest) give a spongious aspect to the bones (Fig. 5A–H). Most of the cortex is formed by a continuously deposited and highly vascularized incipient fibrolamellar bone. The vascularization is plexiform to reticular with incipient and large primary osteons and simple vascular canals (Fig. 5D–F). In the adductor crest area, the vascular canals run parallel to the crest axis and the bone matrix is predominantly parallel-fibered. No growth mark is observed in the cortex of these specimens. There is no evidence of a decrease in vascularization towards the periphery and the bone surface is uneven, suggesting that these bones were still actively growing. An unidentified long bone with a small mid-diaphyseal cross-section diameter has also been sampled (CSl = 1.15 mm; Fig. 5I). The bone wall is thick, compact and is formed of a well-organized bone matrix. The vascularization is reduced and secondary reconstruction is absent. The medullary cavity is well defined and free of bone trabeculae.

TM 85. The mid-diaphyseal cross-section of the radius is incomplete and histological details are poorly preserved (Fig. 5J). Nevertheless, its microstructure is similar to the radius of specimen NMQR 665 (Fig. 4A). The medullary cavity is small, circular and free of bone trabeculae (*k* index of 0.28, RBT of 35.9%, Table 2). A thick ICL consisting of lamellar endosteal bone surrounds the medullary cavity. The cortex is thick and compact, although numerous, large vascular canals are visible (compactness of 0.85, Table 2). Most of the vascular canals are longitudinal primary and secondary osteons. Few radially arranged simple canals are present in a specific region of the cortex (Fig. 5J) and, together with long Sharpey's fibers, attest of a zone of muscle insertion (Fig. 5J,K). In the deep cortex, the osteocyte lacunae are plump and disorganized and, where preserved, the birefringence of the matrix is mostly isotropic under polarized light. The vascularization tends to decrease towards the bone periphery. The bone surface is smooth and a thin layer of lamellar bone with rest lines is visible in the outermost cortex, attesting of a slow down of the growth (Fig. 5L). At the metaphyseal level, the bone wall remains thick and compact although the medullary region is enlarged (*k* index of 0.59; Table 2). The medullary cavity is clearly delimited, but occupied by a few thick bone trabeculae. The structure of the rib section (Fig. 5M) is similar to the rib of NMQR 665. The bone wall is thick, but highly porous. The medullary cavity is not well defined but numerous large erosion cavities are present in the perimedullary region. The structure of the cortex is homogenous and formed by well-vascularized fibrolamellar bone. The osteocyte lacunae are numerous, globular and have a haphazard organization. The vascular canals have a predominantly longitudinal orientation and are mostly primary osteons. The bone surface is uneven and suggests that this bone was still growing at the time of death.

BP/I/1373. Three diaphyseal cross-sections (Fig. 6A), as well as a longitudinal section of the distal epiphysis (Fig. 6B) were prepared from the femur. The histology is poorly preserved, as the birefringence of the bone matrix is partly lost and the sections are damaged by numerous cracks. The serial diaphyseal sections reveal differences in terms of bone compactness. Section I (Fig. 6A(I)) represents the mid-shaft, where the medullary cavity is the smallest (*k* index of 0.10; Table 2). The dorsal part of the cross-section is sub-circular and the ventral part consists of a prominent ridge or adductor crest (Hewison, 2007b). This adductor crest is strongly developed (Table 2), testifying to strong muscle attachment. This femur shows the highest compactness among all the femora sampled in this study (Comp. up to 0.85; Table 2). The medullary cavity is well defined, round, small, and free of bone trabeculae at the mid-diaphyseal level (Fig. 6C). The ICL consists of a layer of endosteally formed lamellar bone that encircles the medullary cavity. The deep cortex is spongious with extensive resorption cavities, especially at the base of the adductor crest (Fig. 6A,C). Because of resorption and poor preservation of the remaining tissue, it is difficult to assess the type of the primary bone matrix in the deep cortex (Fig. 6C). In the outer half of the cortex, the bone consists of an alternation of thin annuli of avascular lamellar bone

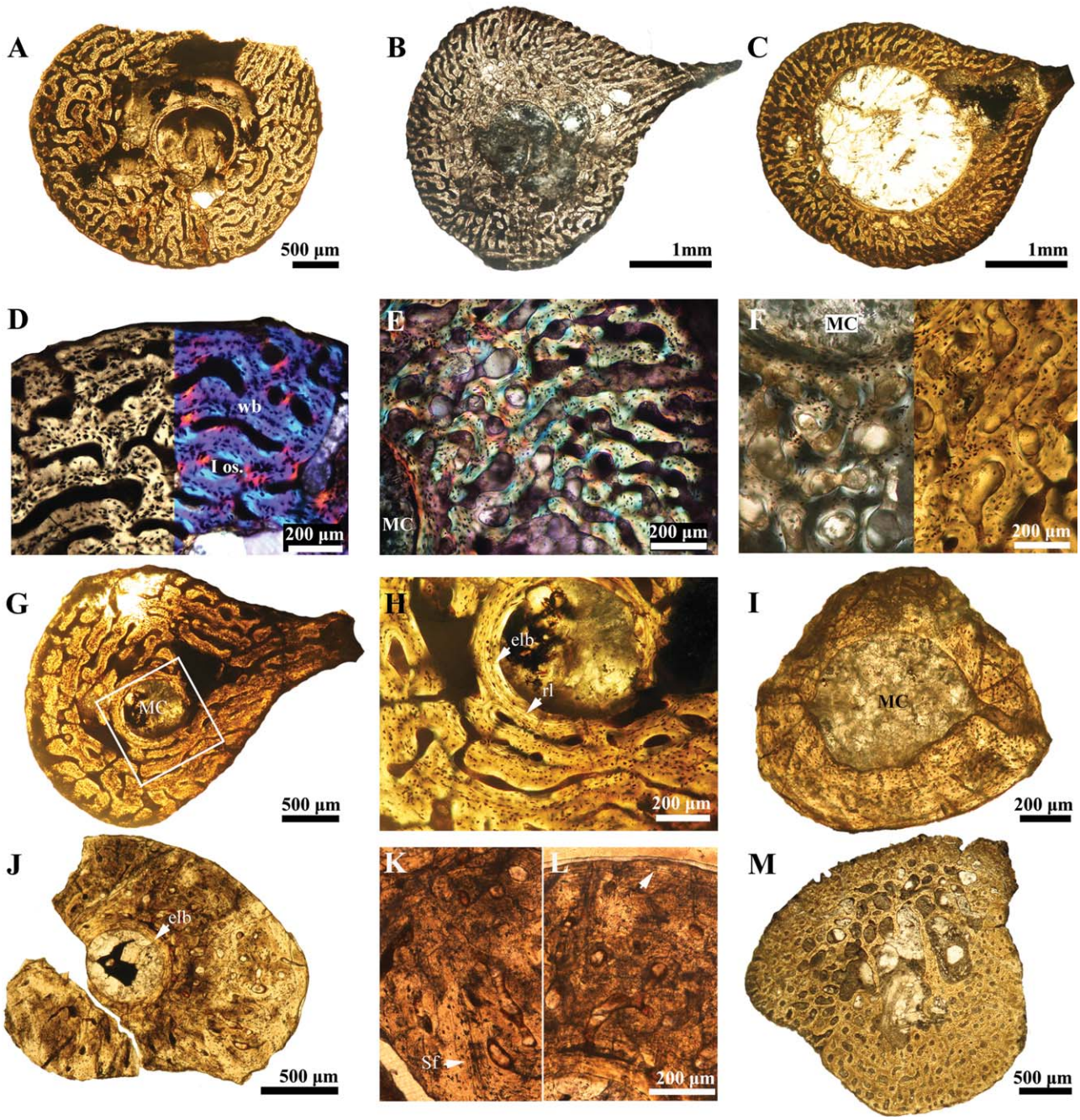

Fig. 5. Bone microstructure of the skeletal elements sampled from specimen TM 186 [femur 1 (A, D), femur 2 (B, C, E, F), femur 3 (G, H) and an unidentified long bone (I)] and TM 85 [radius (J-L) and rib (M)]. (**A**) Mid-diaphyseal cross-section of femur 1. The section is incomplete and the ventral side (adductor crest) is missing. (**B**) Mid-diaphyseal cross-section of femur 2. (**C**) Metaphyseal cross-section of femur 2. (**D**) Higher magnification of the cortex of femur 1 in **A** in normal light (left) and cross-polarized light with lambda compensator (right). The cortex is composed of an incipient fibrolamellar bone. (**E**) Higher magnification of the cortex of femur 2 in **B** in cross-polarized light with lambda compensator. (**F**) Higher magnification of the cortex of the metaphyseal level of femur 2 in **C** in polarized (left) and normal (right) light. (**G**) Mid-diaphyseal cross-section of femur 3. (**H**) Higher magnification of the perimedullary region of femur 3 in **G**. (**I**) Mid-diaphyseal cross-section of an unidentified long bone. (**J**) Mid-diaphyseal cross-section of a radius. (**K**) Higher magnification of the cortex of the radius in **J**. Numerous long Sharpey's fibers are visible in this region (arrow). (**L**) A thin layer of lamellar bone with rest lines (arrow) is visible in the outer most cortex of the radius in **J**. (**M**) Cross-section of a rib. Abbreviations: elb, endosteal lamellar bone; MC, medullary cavity; I os., primary osteon; rl, resorption line; Sf, Sharpey's fibers; wb, woven bone.

and thin zones of woven to parallel-fibered bone (Fig. 6D). Finally, a thick layer of poorly vascularized lamellar bone with closely spaced rest lines is visible in the outermost cortex, all around the section (Fig. 6D,E). The bone surface is smooth and regular suggesting that the growth slowed down already at the time of death. In the

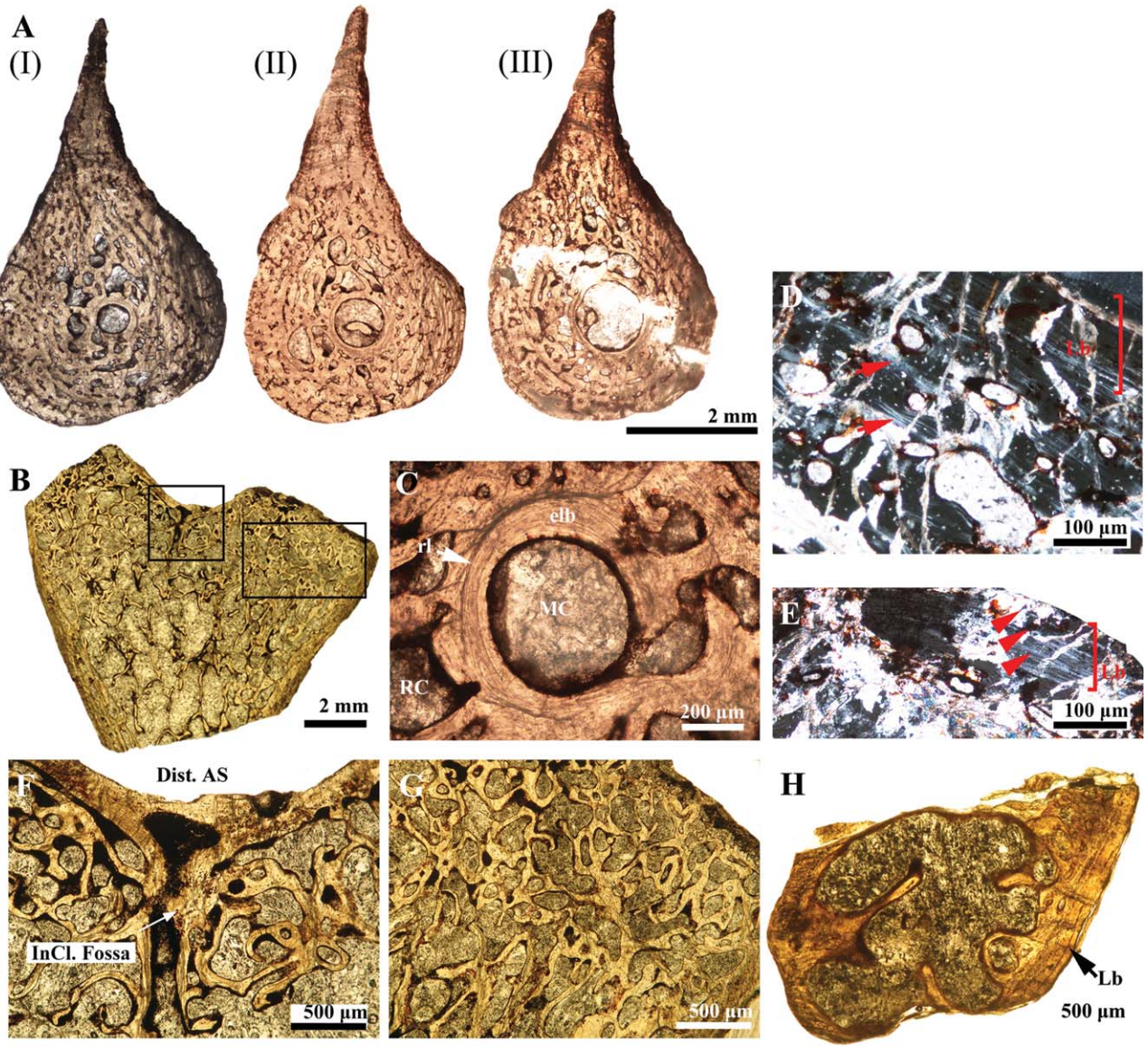

Fig. 6. Bone microstructure of a femur and a rib sampled from specimen BP/I/1373. **(A)** Consecutive cross-sections at the diaphyseal level of a femur (length of 30.8 mm). Note the variability in the bone microanatomy of the different sections I–III. The medullary cavity is the smallest in Section I, which is the closest to the midshaft. **(B)** Longitudinal cross-section of the distal epiphysis of the same femur. **(C)** Higher magnification of the medullary region in **A** (I). The medullary cavity is reduced, but distinct and free of bone trabeculae. A layer of endosteal lamellar bone surrounds the medullary cavity. Large resorption cavities are visible in the perimedullary region. **(D)** Higher magnification of the outer half cortex of the femoral midshaft in polarized light. Note the alternation of thin annuli of lamellar bone (arrows) with thin zones of woven bone. A thick layer of poorly vascularized lamellar bone with closely spaced rest lines is visible in the outermost cortex. **(E)** Thick layer of lamellar bone deposited in the outermost cortex all around the section and interrupted by closely spaced rest lines (arrow heads). **(F)** Higher magnification of the distal articular surface of the femur in **C**. Note that the articular surface is well ossified. The intercondylar fossa is also clearly visible. **(G)** Higher magnification of a condylar region of the distal epiphysis as highlighted in **B**. The bone wall is thin and a dense network of endochondral bony trabeculae fills the medullary region. **(H)** Incomplete cross-section of a rib. The medullary cavity is partially infilled by thick bony trabeculae. Where preserved, the outermost cortex presents a layer of avascular lamellar bone with rest lines. Abbreviations: Dist. AS, distal articular surface; elb, endosteal lamellar bone; InCl. Fossa, intercondylar fossa; Lb, lamellar bone; MC, medullary cavity; RC, resorption cavity; rl, resorption line.

distal epiphysis (Fig. 6B,F,G), the bone wall is relatively thin and becomes thinner towards the articular surface. Most of the bone is filled with a dense mesh of thick bone trabeculae (30–140 µm thick, Fig. 6G). As opposed to the femoral epiphyses of BP/I/5021 (Fig. 3C), BP/I/1373 shows a more robust epiphyseal structure, with a better-ossified articular surface (Fig. 6B,F). Finally, the rib section is incomplete and most of the cortex is missing (CSl = 2.64 mm; Fig. 6H). The medullary cavity was large and filled with a few thick bony trabeculae. Where preserved, the outermost cortex presents a layer of avascular lamellar bone with closely spaced rest lines. All

these features confirm that the largest specimens of our sample consist of mature individuals, most probably adults.

Ontogenetic Variation in the Bone Microstructure of *Lydekkerina*

Femoral microstructure of juvenile individuals. Five femora ranging from 18.7 to 30.8 mm in length were sampled in this study and exhibit ontogenetic variation. Four small femora (ranging from 18.7 to 20 mm in length; BP/I/5021, TM 186) show a bone microstructure characteristic of juvenile and fast growing individuals (Francillion-Vieillot, 1990; Chinsamy-Turan 2005, 2012). The bone wall is relatively thick, highly vascularized and mostly formed of a woven or parallel-fibered bone matrix. The vascular canals consist of incipient primary osteons and simple channels. Secondary reconstruction is limited. The bone surface is uneven and numerous vascular canals are open to the surface. The articular surfaces are not well ossified and the adductor crest is moderately developed. A growth mark represented by a thin annulus of lamellar bone is visible in the inner cortex of at least one specimen suggesting a slow down in the rate of growth. Large erosion cavities are present in the deep cortex and especially at the base of the adductor crest. The medullary cavity is always well delimited, circular and mostly free of bone trabeculae. A thin layer of endosteal lamellar bone usually surrounds the medullary region.

Femoral microstructure of the adult individual. In the largest specimen (femoral length of 30.8 mm; BP/I/1373), the bone microstructure is congruent with a mature individual for which the growth slowed down. The adductor crest is well developed and thus more prominent than in smaller individuals, and the articular surfaces of the bone are better ossified. The bone surface is even and the outermost cortex formed by a thick layer of lamellar bone with rest lines. In this adult individual, the medullary cavity is proportionally smaller than in younger individuals and the midshaft section is more compact (k index = 0.10, compactness = 0.85). This relative compaction of the midshaft during ontogeny is due to the limited expansion of the medullary cavity, the centripetal deposition of lamellar endosteal bone in the vascular spaces, the further deposition of periosteal bone, as well as the decrease in vascularization toward the periphery.

Histological variation in the skeleton. Even though, the general microstructure is consistent between the bones sampled, some variability is observed among long bones at the mid-diaphyseal level. All sampled long bones exhibit thick cortices with reduced, but well-defined medullary cavities, mostly free of bony trabeculae and bordered by a layer of endosteally formed lamellar bone, suggesting limited expansion of the medullary cavity during ontogeny. In the stylopod (humerus, femur), most of the deep cortical bone is well-vascularized and large erosion cavities occupy the perimedullary region. The cortical vascularization, as well as resorption in the perimedullary region (at least at the mid-diaphyseal level), is less dense in the zeugopod elements (here the radius and ulna) than in the stylopod ones. Several ribs have been sampled and exhibit variable microanatomy. The histology of the various bones studied, indicates that some individuals experienced a sustained fast growth early in ontogeny, whereas others faced periodic slow down of the growth (represented by thin annuli of lamellar bone) before the attainment of sexual maturity. For example, BP/I/5021 with a femoral length of 18.7 mm and a mid-diaphyseal width (CSw, see Table 2) of 2.24 mm shows an annulus in the inner cortex, while no growth marks are visible in the larger femora from TM 86. The same applies to both radii sectioned. The radius from NMQR 665 exhibits at least 2 annuli, while the similar-sized radius from TM 85 seems to show uninterrupted growth until sexual maturity.

Lifestyle Inference Using Quantitative Models

The mid-diaphyseal cross-sections of the radii of specimens NMQR 665 and TM 85, as well as the Sections 1 and 2 of the femur of specimen BP/I/1373 have been analyzed in Bone Profiler in order to extract various compactness profile parameters (for more details see Girondot and Laurin, 2003; Canoville and Laurin, 2010; Table 3). The lifestyle inference models of Germain and Laurin (2005) and Quemeneur et al. (2013) have been applied to these sections. *Lydekkerina* is inferred to have been amphibious or aquatic based on its radial and femoral microanatomy (Table 3).

DISCUSSION

Several paleohistological studies have been conducted on Permo-Triassic temnospondyls (Enlow and Brown, 1956; Ricqlès, 1979; Damiani, 2000; Laurin et al., 2004; Ricqlès et al., 2004; Steyer et al., 2004; Sanchez et al., 2008; Ray et al., 2009; Mukherjee et al., 2010; Sanchez et al., 2010; Witzmann and Soler Gijón, 2010; McHugh, 2012; Konietzko-Meier and Klein, 2013; Konietzko-Meier et al., 2013; Konietzko-Meier and Sander, 2013; Konietzko-Meier and Schmitt, 2013; Sanchez and Schoch, 2013; McHugh, 2014), but few included Early Triassic amphibian material (Damiani, 2000, Ray et al., 2009; Mukherjee et al., 2010; McHugh, 2012) and even fewer have focused on Karoo Basin taxa (McHugh, 2012, 2014). Besides being the first comprehensive work on *Lydekkerina*'s bone microstructure, the current study contributes to the better understanding of the paleobiology of Early Triassic amphibians, and sheds new light on the convergent adaptive strategies of the continental tetrapod fauna to the harsh post Permian-extinction environment of the Karoo Basin.

General Paleobiological Inferences for *Lydekkerina*

Inferred ontogenetic stages versus body size variability in the fossil record. Previous studies of *Lydekkerina* concluded that most of the specimens found in the fossil record are subadult or fully-grown individuals, usually with midline skull lengths between 60 to 80 mm (Shishkin et al., 1996; Hewison, 2007a). Moreover, Jeannot et al., (2006) suggested that the *L. huxleyi* holotype was already a small adult with a skull length

TABLE 3. Inferred lifestyle for *Lydekkerina* according to the models of Germain and Laurin (2005) on the radius and Quemeneur et al. (2013) on the femur

Germain and Laurin, 2005—Ternary model			Quemeneur et al., 2013—Ternary model		
Parameters	Radius NMQR 665 Diaphyseal section	Radius TM 85 Diaphyseal section	Parameters	Femur BP/I/1373 Diaphyseal section I	Femur BP/I/1373 Diaphyseal section II
MD (mm)	2.03	1.99	R_{Min}	0.405	0
Comp.	0.83	0.847	S	0.153	0.184
S	0.08	0.029	R_{Max}	0.993	0.983
P	0.34	0.269	M Comp.	0.846	0.786
Min	0	0	Min	0.471	0
			O Comp.	0.847	0.786
			SVL (cm)	30-60	30–60
Inferred lifestyle	Amphibious	Amphibious	Inferred lifestyle	Aquatic	Amphibious

See these publications for details on the inference models, as well as the parameters S, P, Min, Max, R_{Min}, and R_{Max} obtained in Bone Profiler (Girondot and Laurin, 2003). *Lydekkerina* was estimated to reach an adult snout-vent length of 30–60 cm. This broad estimate is based on the reconstruction of Watson (1920) and a comparison with the body proportions of the largest lydekkerinid *Eolydekkerina* (Shishkin et al., 1996; Jeannot et al., 2006).
Abbreviations: Comp., compactness; M Comp., modeled compactness (in Bone Profiler); MD, maximal diameter of the section; O Comp., observed compactness; SVL, snout-vent length.

of 58.4 mm. Bone histology clearly showed that our sample contains juvenile individuals still actively growing at the time of death. This was expected for the specimen BP/I/5021, which exhibits an estimated skull length of 49 to 54.4 mm, well within the range of the smallest skulls known in the fossil record for this species. Specimen TM 186 contains six skulls ranging in length from ~62–67 mm; considering previous hypotheses, these individuals could have been *a priori* regarded as adults. However, bone histology demonstrates that the femora sampled for this specimen were still actively growing and therefore belonged to juvenile individuals.

The study of *Lydekkerina* bone microstructure reveals that there are more juvenile individuals in the fossil record than previously ascribed to in the literature. Indeed, bone histology permitted the identification of individuals that were still actively growing at the time of death, but were previously considered to be mature based on skull length. Here, we show that some individuals (TM 186) with skull sizes above 62 mm exhibit femora that are still actively growing although a smaller specimen (BP/I/5022) exhibits a humerus and a rib for which the growth slowed down already. These results contradict the assumptions of Shishkin et al., (1996) and Hewison (2007a) that most of the specimens of *Lydekkerina* recovered were adult or mature individuals. Moreover, the incoherence between skull size and apparent ontogenetic stage could be explained by body size variability for *Lydekkerina* adult specimens due to inherent plasticity in growth (see below) or sexual dimorphism.

Bone growth patterns. Previous studies revealed that the different groups of temnospondyls showed different growth strategies with predominance for a cyclical and rather slow growth pattern, with deposition of parallel fibered to lamellar periosteal bone interrupted by numerous growth marks (annuli or LAGs) (Ricqlès, 1979; Mukherjee et al., 2010; Konietzko-Meier and Klein, 2013; McHugh, 2014). Most of the studied taxa, whether they were large or small, grew over several years before attaining sexual maturity and therefore experienced a protracted juvenile period. Some groups, especially from the Triassic, showed a periodic or sustained high initial growth with deposition of fibrolamellar bone (Mukherjee et al., 2010; Konietzko-Meier and Klein, 2013; Konietzko-Meier and Sander, 2013; Konietzko-Meier and Schmitt, 2013).

The deposition of incipient fibrolamellar bone or well-vascularized parallel-fibered bone tissue in juvenile individuals of *Lydekkerina* indicates relatively faster growth rates during early ontogeny. The attainment of sexual maturity is marked by a slow down in growth and the further deposition of lamellar bone with rest lines in the outer cortex of adults. However, it appears that the duration of the early growth to sexual maturity was variable among individuals. Indeed some specimens exhibited azonal compacta, while others showed periodic slow down in growth (as evidenced by the narrow deposits of annuli), although unlike most other temnospondyls no lines of arrested growth were observed, indicating no cessation of growth before the attainment of sexual maturity. In conjunction with an apparent poor correlation between ontogenetic stage and body size, this flexibility in growth could be explained by developmental plasticity for this species (e.g., Starck and Chinsamy 2002; Sander and Klein, 2005). Such flexibility in development has previously been described for temnospondyls (Sanchez and Schoch, 2013) and could result from variable responses to environmental stress encountered during an individual's life. A study on modern amphibians also showed that species inhabiting unpredictable environments have a greater developmental plasticity than species living in stable habitats (Richter-Boix et al., 2006). These results of an early fast growth, with an apparent short juvenile period are congruent with a small body size for this species and support the hypothesis proposed by several authors (Shishkin and Rubidge, 2000; Schoch and Rubidge, 2005; Hewison, 2007a) of a truncated ontogenetic trajectory.

The deposition of incipient fibrolamellar bone early in ontogeny was initially observed in small-sized trematosaurids from the Panchet Formation, India, by Ray

et al., (2009) and Mukherjee et al., (2010). Fibrolamellar bone has been also described in *Micropholis* and *Lyddekerina* from the Katberg Formation, South Africa (McHugh, 2012; and in the present study). All these genera are recovered from the Early Triassic and regarded as small bodied-forms as compared to their closest relatives. The fibrolamellar bone tissues in these animals indicate rapid rates of growth and the small body sizes suggest shortened developmental time to sexual maturity, as compared to other temnospondyls. This growth strategy could reflect an adaptation to survive the dry, unpredictable environmental conditions of the Early Triassic (Robinson, 1967; Smith and Ward, 2001; Pace et al., 2009; Mukherjee et al., 2010; Smith et al., 2012) by maintaining large breeding populations (Hewison, 2007a, 2007b).

Bone microanatomy and lifestyle adaptations. Temnospondyls were morphologically and ecologically diverse with dwarf to giant forms inhabiting terrestrial, riverine, lacustrine, and even marine environments (Schoch, 2009, 2014; Fortuny et al., 2011). Previous works showed that aquatic temnospondyls exhibit either osteosclerotic (compact) or osteoporotic (spongious) cortices (Sanchez et al., 2010; Steyer et al., 2014) usually interpreted as adaptations for bottom dwelling or active swimming behavior in the water column, respectively (Ricqlès and Buffrénil, 2001). In these taxa, the medullary cavity is filled with a dense network of bone trabeculae and the transition between the medullary region and the cortical bone is often inconspicuous. Moreover, calcified cartilage is sometimes present within the trabeculae (Ricqlès and Buffrénil, 2001; Sanchez et al., 2010; Sanchez and Schoch, 2013). Some temnospondyls, inferred as partially terrestrial, showed a clear transition between the medulla and the cortex, associated with the absence of calcified cartilage retention in the midshaft (Sanchez et al., 2008; Mukherjee et al., 2010; McHugh, 2012). This is for example the case in some Early Triassic trematosaurid from India (Mukherjee et al., 2010). Nevertheless, the humerus and femur of these taxa exhibit a medullary cavity infilled by bone trabeculae. This adaptation to terrestriality has also been attributed to *Micropholis*, a small amphibamid temnospondyl from the *Lystrosaurus* AZ of South Africa, on the basis of anatomical, taphonomic, and bone microstructural features (Hewison, 1996; Schoch and Rubidge, 2005; McHugh, 2012). The humerus of this species has a well-defined and vacant medullary cavity and the bone cortex is relatively thick and compact.

The thick and rather compact cortex of the long bones of *Lydekkerina*'s mature specimens, associated with a reduced medullary cavity, suggest that *Lydekkerina* may have been adapted to aquatic environments, as tetrapods inhabiting shallow water and being bottom dwellers exhibit osteosclerotic bones (Ricqlès and Buffrénil, 2001; Laurin et al., 2004; Canoville and Laurin, 2009, 2010; Quemeneur et al., 2013; Sanchez and Schoch, 2013). This is supported by the results of both inference models (Germain and Laurin, 2005; Quemeneur et al., 2013) that give an aquatic to amphibious lifestyle for *Lydekkerina*. However, these results should be considered cautiously, since these inference models are based on amniotes whereas temnospondyls are non-amniotes (Quemeneur et al., 2013). Such compact long bones, with a RBT generally superior to 30%, are also found in some fossorial animals (Botha and Chinsamy, 2004; Botha-Brink and Angielczyk, 2010; Nasterlack et al., 2012; Straehl et al., 2013).

However, *Lydekkerina*'s limb bones, unlike aquatic temnospondyls, exhibit a well defined medullary cavity, free of bone trabeculae at the mid-diaphyseal level. This feature is typical of terrestrial tetrapods (Canoville and Laurin, 2010). Other characteristics denote a significant terrestrial mode of existence, such as a strongly developed adductor crest for muscle attachments and relatively well-ossified epiphyses of the femur at the adult stage, as well as no remnant of calcified cartilage in the long bone diaphyses.

In summary, *Lydekkerina* exhibits microanatomical and morphological features implying a terrestrial locomotion. This amphibian may have inhabited ephemeral water ponds, as revealed by its thick bone walls. However, it was able to move on dry land to search for other pools or to take refuge, for example, in therapsid burrows during the periods of droughts of the Early Triassic (Smith et al., 2012). An occasional burrowing lifestyle, as suggested by Hewison (2007b) can not be excluded based on bone microstructure. According to Smith et al., (2012) there is a preferential preservation of amphibious or fossorial animals in the Early Triassic Karoo Basin and this taphonomic bias may explain the abundance of *Lydekkerina*, often found in clusters (Hewison, 1996; Pawley and Warren, 2005). Nevertheless, the articulated remains of the small Early Triassic amphibians such as *Broomistega, Micropholis*, and *Lydekkerina* have often been found in association with other terrestrial and burrowing animals such as *Thrinaxodon*, *Lystrosaurus, or Procolophon* (Hewison, 1996; Chinsamy-Turan, 2012; Fernandez et al., 2013). The burrowing behavior of Triassic amphibians could have been only opportunistic when the climatic conditions were unfavorable (Abdala et al., 2006; Fernandez et al., 2013).

Adaptation to Harsh Environmental Conditions in the Early Triassic of the Karoo Basin

While many tetrapod taxa became extinct as the Permian ended, few groups survived into the Triassic and prospered (Smith and Botha, 2005; Smith et al., 2012). Why did some taxa survive while others faced demise? Considering bone microstructure, taphonomic, and anatomical data, there appears to be consensus that peculiar lifestyles and growth strategies enhanced survival in the unpredictable conditions of the post-extinction Early Triassic (e.g., Ray and Chinsamy, 2004; Smith and Botha, 2005; Botha-Brink and Angielczyk, 2010; Huttenlocker and Botha-Brink, 2013).

Over the last decade, the number of bone microstructural studies on Permo-Triassic tetrapods from the Karoo Basin increased exponentially, enabling a better understanding of their paleobiology. Nevertheless, these studies mainly focused on the better known mammal-like reptiles or therapsids (e.g., Botha and Chinsamy, 2000, 2004, 2005; Ray and Chinsamy, 2004; Ray et al., 2004, 2005; Botha and Angielczyk, 2007; Chinsamy-Turan, 2012; Nasterlack et al., 2012; Huttenlocker and Botha-Brink, 2013) and to a lesser extent on parareptiles (Scheyer and Sander, 2009; Botha-Brink and Smith,

2012) and archosauromorphs (Botha-Brink and Smith, 2011). Few studies focused on amphibians (McHugh, 2012, 2014), which were a significant component of the continental fauna (Damiani, 2003; Smith et al., 2012). On the basis of bone microstructure, several studies reported that Permo-Triassic taxa, pertaining to taxonomically and morphologically diverse groups (from large therapsids to small parareptiles), had digging adaptations to cope with prolonged periods of drought (Ray and Chinsamy, 2004; Botha and Chinsamy, 2004, 2005; Botha-Brink and Smith, 2012; Nasterlack et al., 2012). This hypothesis of a widespread fossorial behavior was also supported by the large number and diversity of burrow casts found in the Late Permian and the Early Triassic of the Karoo Basin (Smith, 1987; Groenewald et al., 2001; Bordy et al., 2011). These burrows sometimes even contained the remains of their inhabitants (Smith, 1987; Damiani et al., 2003; DeBraga, 2003; Abdala et al., 2006; Fernandez et al., 2013; Botha-Brink, 2014). Simultaneously, independent histological studies showed that some taxa that survived the end-Permian extinction event, as well as the tetrapods that were abundant in the Early Triassic shared similar, unusual growth patterns (Ray et al., 2005; Botha-Brink and Angielczyk, 2010; Botha-Brink and Smith, 2011; Huttenlocker and Botha-Brink, 2013), associated with a shortened development and thus body size reduction (Huttenlocker and Botha-Brink, 2013, 2014). These taxonomically diverse tetrapods all exhibited a faster growth early in ontogeny as compared to their closest relatives (e.g., Botha-Brink and Smith, 2011; Huttenlocker and Botha-Brink, 2013). It therefore appears that a faster growth rate to reach sexual maturity is a consistent adaptation for taxa enduring harsh environmental conditions (Chinsamy and Hurum 2006; Botha-Brink and Smith, 2011).

This study constitutes the first extensive osteohistological assessment of the small stereospondyl *Lydekkerina huxleyi*. Our results confirm that this amphibian resorted to convergent adaptations to other drought tolerant therapsids, parareptiles and archosauromorphs. Thus, besides its apparent plasticity in growth, *Lydekkerina* had higher growth rates to sexual maturity as compared to most other temnospondyls. In addition, its ability to be more terrestrial enabled *Lydekkerina* to survive and prosper during the episodic droughts and unpredictable environment of the Early Triassic.

CONCLUSIONS

1. Histological assessment suggests that contrary to previous hypotheses, there are more juvenile or immature specimens of *Lydekkerina* in the fossil record.
2. Despite exhibiting plasticity in growth, *Lydekkerina* experienced an overall faster growth during early ontogeny (thereby attaining sexual maturity sooner), as compared to most temnospondyls.
3. The microanatomy of the long bones, with their thick bone walls and distinctive vacant medullary cavity suggests that *Lydekkerina* may have been amphibious with a tendency to be more terrestrial than its closest relatives, i.e. most stereospondyls. Taphonomy and bone histology suggests that it may have occasionally exploited a fossorial lifestyle.

ACKNOWLEDGEMENTS

The authors are thankful to the following curators who facilitated access to the amphibian material and for providing specimens for histological sections: Sheena Kaal (Collection Manager, Iziko South African Museum, Cape Town), Roger Smith (Curator, Iziko South African Museum, Cape Town), Bernhard Zipfel (Curator, Evolutionary Studies Institute, University of the Witwatersrand, Johannesburg), Heidi Fourie (Ditsong National Museum of Natural History, Pretoria), Jennifer Botha-Brink and Elize Butler (Bloemfontein). Zaituna Erasmus (Iziko South African Museum, Cape Town) is acknowledged for having especially prepared some specimens. We thank two anonymous reviewers for comments that improved the manuscript. The Claude Leon Foundation and the National Research Foundation of South Africa are acknowledged for research support for A. Canoville and A. Chinsamy-Turan, respectively.

LITERATURE CITED

Abdala F, Cisneros JC, Smith RM. 2006. Faunal aggregation in the Early Triassic Karoo Basin: earliest evidence of shelter-sharing behavior among tetrapods? Palaios 21:507–512.

Bordy EM, Sztano O, Rubidge BS, Bumby A. 2011. Early Triassic vertebrate burrows from the Katberg Formation of the southwestern Karoo Basin, South Africa. Lethaia 44:33–45.

Botha J, Chinsamy A. 2000. Growth patterns deduced from the bone histology of the cynodonts *Diademodon* and *Cynognathus*. J Vert Paleontol 20:705–711.

Botha J, Chinsamy A. 2004. Growth and life habits of the Triassic cynodont *Trirachodon*, inferred from bone histology. Acta Palaeontol Pol 49:619–627.

Botha J, Chinsamy A. 2005. Growth patterns of *Thrinaxodon liorhinus*, a non-mammalian cynodont from the Lower Triassic of South Africa. Palaeontology 48:385–394.

Botha J, Angielczyk KD. 2007. An integrative approach to distinguishing the Late Permian dicynodont species *Oudenodon bainii* and *Tropidostoma microtrema* (Therapsida: Anomodontia). Palaeontology 50:1175–1209.

Botha-Brink J. 2014. The lifestyle of Permo-Triassic *Lystrosaurus*. J Vert Paleontol:95.

Botha-Brink J, Angielczyk KD. 2010. Do extraordinarily high growth rates in Permo-Triassic dicynodonts (Therapsida, Anomodontia) explain their success before and after the end-permian extinction? Zool J Linn Soc 160:341–365.

Botha-Brink J, Smith RMH. 2011. Osteohistology of the Triassic archosauromorphs *Prolacerta*, *Proterosuchus*, *Euparkeria*, and *Erythrosuchus* from the Karoo Basin of South Africa. J Vert Paleontol 31:1238–1254.

Botha-Brink J, Smith RMH. 2012. Palaeobiology of Triassic procolophonids, inferred from bone microstructure. CR Palevol 11:419–433.

Broili F, Schröder HC. 1937. Beobachtungen an wirbeltieren der Karrooformation. XXV. Über *Micropholis huxleyi*. XXVI. Über *Lydekkerina* Broom. Sitzungsberichte der Bayerischen Akademie der Wissenschaften: 19–57.

Canoville A, Laurin M. 2009. Microanatomical diversity of the humerus and lifestyle in lissamphibians. Acta Zool 90:110–122.

Canoville A, Laurin M. 2010. Evolution of humeral microanatomy and lifestyle in amniotes, and some comments on palaeobiological inferences. Biol J Linn Soc 100:384–406.

Castanet J, Caetano MH. 1995. Influence du mode de vie sur les caractéristiques pondérales et structurales du squelette chez les amphibiens anoures. Can J Zool 73:234–242.

Catuneanu O, Wopfner H, Eriksson PG, Cairncross B, Rubidge BS, Smith RMH, Hancox PJ. 2005. The Karoo Basins of south-central Africa. J Afr Earth Sci 43:211–253.

Chinsamy A, Hurum J. 2006. Bone microstructure and growth patterns of early mammals. Acta Palaeontol Pol 51:325–338.

Chinsamy A, Raath MA. 1992. Preparation of fossil bone for histological examination. Palaeont Afr 29:39–44.

Chinsamy-Turan A. 2005. The microstructure of dinosaur bone: deciphering biology with fine-scale techniques. Baltimore: Johns Hopkins University Press.

Chinsamy-Turan A. 2012. Forerunners of mammals: radiation, histology, biology. Bloomington: Indiana University Press.

Currey JD, Alexander R. 1985. The thickness of the walls of tubular bones. J Zool 206:453–468.

Damiani RJ. 2000. Bone histology of some Australian Triassic temnospondyl amphibians: preliminary data. Mod Geol 24:109–124.

Damiani RJ. 2003. Temnospondyls from the Beaufort Group (Karoo Basin) of South Africa and their biostratigraphy. Gondwana Res 7:165–173.

Damiani R, Modesto S, Yates A, Neveling J. 2003. Earliest evidence of cynodont burrowing. Proc R Soc B 270:1747–1751.

Debraga M. 2003. The postcranial skeleton, phylogenetic position, and probable lifestyle of the Early Triassic reptile *Procolophon trigoniceps*. Can J Earth Sci 40:527–556.

Enlow DH, Brown SO. 1956. A comparative histological study of fossil and recent bone tissues. Part I. Tex J Sci 8:405–444.

Fernandez V, Abdala F, Carlson KJ, Rubidge BS, Yates A, Tafforeau P. 2013. Synchrotron reveals Early Triassic odd couple: injured amphibian and aestivating therapsid share burrow. Plos One 8: e64978.

Fortuny J, Marcé-Nogué J, de Esteban-Trivigno S, Gil L, Galobart A. 2011. Temnospondyli bite club: ecomorphological patterns of the most diverse group of early tetrapods. J Evol Biol 24:2040–2054.

Francillion-Vieillot H, Buffrénil de V, Castanet J, Géraudie J, Meunier FJ. 1990. Microstructure and mineralization of vertebrate skeletal tissues. In: Carter JG, editor. Skeletal biomineralization: patterns, processes and evolutionary trends. New York: Van Nostrand. p 471–529.

Germain D, Laurin M. 2005. Microanatomy of the radius and lifestyle in amniotes (Vertebrata, Tetrapoda). Zool Scr 34:335–350.

Girondot M, Laurin M. 2003. Bone Profiler: a tool to quantify, model, and statistically compare bone-section compactness profiles. J Vert Paleontol 23:458–461.

Groenewald GH, Welman J, MacEachern JA. 2001. Vertebrate burrow complexes from the Early Triassic *Cynognathus* zone (Driekoppen Formation, Beaufort Group) of the Karoo Basin, South Africa. Palaios 16:148–160.

Hewison RH. 1996. The skull of *Deltacephalus whitei*, a lydekkerinid temnospondyl amphibian from the Lower Triassic of Madagascar. Palaeontology 39:305–321.

Hewison RH. 2007a. The skull and mandible of the stereospondyl *Lydekkerina huxleyi*, (Tetrapoda: Temnospondyli) from the Lower Triassic of South Africa, and a reappraisal of the family Lydekkerinidae, its origin, taxonomic relationships and phylogenetic importance. J Temnospondyl Palaeontol 1:1–80.

Hewison RH. 2007b. The sacral region, pelvis and hind limb of the stereospondyl *Lydekkerina huxleyi* (Tetrapoda: Temnospondyli) from the Lower Triassic of South Africa. J Temnospondyl Palaeontol 2:1–28.

Huttenlocker AK, Botha-Brink J. 2013. Body size and growth patterns in the therocephalian *Moschorhinus kitchingi* (Therapsida: Eutheriodontia) before and after the end-Permian extinction in South Africa. Paleobiology 39:253–277.

Huttenlocker AK, Botha-Brink J. 2014. Bone microstructure and the evolution of growth patterns in Permo-Triassic therocephalians (Amniota, Therapsida) of South Africa. Peer J 2:e325.

Jeannot AM, Damiani R, Rubidge B. 2006. Cranial anatomy of the Early Triassic stereospondyl *Lydekkerina huxleyi* (Tetrapoda: Temnospondyli) and the taxonomy of South African lydekkerinids. J Vert Paleontol 26:822–838.

Kammerer CF, Angielczyk KD, Fröbisch J, editors. 2014. Early evolutionary history of the Synapsida, vertebrate paleobiology and paleoanthropology series. Netherlands: Springer.

Kemp TS. 2005. The origin and evolution of mammals.Oxford: Oxford University Press.

Konietzko-Meier D, Klein N. 2013. Unique growth pattern of *Metoposaurus diagnosticus krasiejowensis* (Amphibia, Temnospondyli) from the Upper Triassic of Krasiejów, Poland. Palaeogeogr Palaeoclimatol Palaeoecol 370:145–157.

Konietzko-Meier D, Sander PM. 2013. Long bone histology of *Metoposaurus diagnosticus* (Temnospondyli) from the Late Triassic of Krasiejów (Poland) and its paleobiological implications. J Vert Paleontol 33:1003–1018.

Konietzko-Meier D, Schmitt A. 2013. A histological study of a femur of *Plagiosuchus*, a Middle Triassic temnospondyl amphibian from southern Germany, using thin sections and micro-CT scanning. Neth J Geosci 92:97–108.

Konietzko-Meier D, Bodzioch A, Sander PM. 2013. Histological characteristics of the vertebral intercentra of *Metoposaurus diagnosticus* (Temnospondyli) from the Upper Triassic of Krasiejow (Upper Silesia, Poland). T Roy Soc Edin Earth 103:1–14.

Laurin M, Canoville A, Germain D. 2011. Bone microanatomy and lifestyle: a descriptive approach. CR Palevol 10:381–402.

Laurin M, Girondot M, Loth M-M. 2004. The evolution of long bone microstructure and lifestyle in lissamphibians. Paleobiology 30: 589–613.

McHugh JB. 2012. Temnospondyl ontogeny and phylogeny, a window into terrestrial ecosystems during the Permian-Triassic mass extinction. PhD Dissertation, University of Iowa.

McHugh JB. 2014. Paleohistology and histovariability of the Permian stereospondyl *Rhinesuchus*. J Vert Paleontol 34:59–68.

Mukherjee D, Ray S, Sengupta DP. 2010. Preliminary observations on the bone microstructure, growth patterns, and life habits of some Triassic temnospondyls from India. J Vert Paleontol 30:78–93.

Nasterlack T, Canoville A, Chinsamy A. 2012. New insights into the biology of the Permian genus *Cistecephalus* (Therapsida, Dicynodontia). J Vert Paleontol 32:1396–1410.

Pace DW, Gastaldo RA, Neveling J. 2009. Early Triassic aggradational and degradational landscapes of the Karoo Basin and evidence for climate oscillation following the P-tr event. J Sediment Res 79:316–331.

Padian K, Lamm ET. 2013. Bone histology of fossil Tetrapods: advancing methods, analysis, and interpretation. California: University of California Press.

Pawley K, Warren A. 2004. Immaturity vs paedomorphism: a rhinesuchid stereospondyl postcranium from the Upper Permian of South Africa. Palaeont Afr 40:1–10.

Pawley K, Warren A. 2005. A terrestrial stereospondyl from the Lower Triassic of South Africa: the postcranial skeleton of *Lydekkerina huxleyi* (Amphibia: Temnospondyli). Palaeontology 48:281–298.

Quemeneur S, Buffrénil V, Laurin M. 2013. Microanatomy of the amniote femur and inference of lifestyle in limbed vertebrates. Biol J Linn Soc 109:644–655.

Ray S, Botha J, Chinsamy A. 2004. Bone histology and growth patterns of some nonmammalian therapsids. J Vert Paleontol 24: 634–648.

Ray S, Chinsamy A. 2004. *Diictodon feliceps* (Therapsida, Dicynodontia): bone histology, growth, and biomechanics. J Vert Paleontol 24:180–194.

Ray S, Chinsamy A, Bandyopadhyay S. 2005. *Lystrosaurus murrayi* (Therapsida, Dicynodontia): bone histology, growth and lifestyle adaptations. Palaeontology 48:1169–1185.

Ray S, Mukherjee D, Bandyopadhyay S. 2009. Growth patterns of fossil vertebrates as deduced from bone microstructure: case studies from India. J Biosci 34:661–672.

Richter-Boix A, Llorente GA, Montori A. 2006. A comparative analysis of the adaptive developmental plasticity hypothesis in six mediterranean anuran species along a pond permanency gradient. Evol Ecol Res 8:1139–1154.

Ricqlès A de . 1979. Relations entre structures histologiques, ontogenèse, stratégies démographiques et modalités évolutives: le cas des reptiles captorhinomorphes et des stégocéphales temnospondyles. CR Acad Sci 288:1147–1150.

Ricqlès A de . 2011. Vertebrate palaeohistology: past and future. CR Palevol 10:509–515.

Ricqlès de A, Buffrénil de V. 2001. Bone histology, heterochronies and the return of tetrapods to life in water: where are we? In: Mazin JM, Buffrénil de V, editors. Secondary adaptation of tetrapods to life in water. München: Verlag Dr. Friedrich Pfeil. p 289–310.

Ricqlès A de , Castanet J, Francillon-Vieillot H. 2004. The 'message' of bone tissue in paleoherpetology. Ital J Zool 1:3–12.

Robinson PL. 1967. The Indian Gondwana Formations—a review. In: Proceedings of 1st IUGS International Symposium on Gondwana Stratigraphy and Paleontology, Mar del Plata, Argentina. p 201–268.

Rubidge B. 2013. The roots of early mammals lie in the Karoo: Robert Broom's foundation and subsequent research progress. Trans R Soc S Afr 68:41–52.

Sanchez S, Germain D, Ricqlès A, de Abourachid A, Goussard F, Tafforeau P. 2010. Limb-bone histology of temnospondyls: implications for understanding the diversification of palaeoecologies and patterns of locomotion of Permo-Triassic tetrapods. J Evol Biol 23: 2076–2090.

Sanchez S, Klembara J, Castanet J, Steyer JS. 2008. Salamander-like development in a seymouriamorph revealed by palaeohistology. Biol Lett 4:411–414.

Sanchez S, Schoch RR. 2013. Bone histology reveals a high environmental and metabolic plasticity as a successful evolutionary strategy in a long-lived homeostatic Triassic temnospondyl. Evol Biol 40:627–647.

Sander PM, Klein N. 2005. Developmental plasticity in the life history of a prosauropod dinosaur. Science 310:1800–1802.

Scheyer TM, Sander PM. 2009. Bone microstructures and mode of skeletogenesis in osteoderms of three pareiasaur taxa from the Permian of South Africa. J Evol Biol 22:1153–1162.

Schoch RR. 2009. Evolution of life cycles in early amphibians. Annu Rev Earth Planet Sci 37:135–162.

Schoch RR. 2014. Life cycles, plasticity and palaeoecology in temnospondyl amphibians. Palaeontology 57:517–529.

Schoch RR, Rubidge BS. 2005. The amphibamid *Micropholis* from the *Lystrosaurus* Assemblage Zone of South Africa. J Vert Paleontol 25:502–522.

Shishkin MA, Rubidge BS. 2000. A relict rhinesuchid (Amphibia: Temnospondyli) from the Lower Triassic of South Africa. Palaeontology 43:653–670.

Shishkin MA, Rubidge BS, Kitching JW. 1996. A new Lydekkerinid (Amphibia, Temnospondyli) from the Lower Triassic of South Africa: implications for evolution of the early capitosauroid cranial pattern. Phil Trans R Soc B 351:1635–1659.

Smith RM. 1987. Helical burrow casts of therapsid origin from the Beaufort Group (Permian) of South Africa. Palaeogeogr Palaeoclimatol Palaeoecol 60:155–169.

Smith R, Botha J. 2005. The recovery of terrestrial vertebrate diversity in the South African Karoo Basin after the end-Permian extinction. CR Palevol 4:623–636.

Smith R, Rubidge B, van der Walt M. 2012. Therapsid biodiversity patterns and paleoenvironments of the Karoo Basin, South Africa. In: Chinsamy-Turan A, editor. Forerunners of mammals—radiation, histology, biology. Bloomington and Indianapolis: Indiana University Press. p 31–62.

Smith RMH, Ward PD. 2001. Pattern of vertebrate extinctions across an event bed at the Permian-Triassic boundary in the Karoo Basin of South Africa. Geology 29:1147–1150.

Starck JM, Chinsamy A. 2002. Bone microstructure and developmental plasticity in birds and other dinosaurs. J Morphol 254: 232–246.

Steyer JS. 2002. The first articulated trematosaur 'amphibian' from the Lower Triassic of Madagascar: implications for the phylogeny of the group. Palaeontology 45:771–793.

Steyer JS. 2003. A revision of the Early Triassic "Capitosaurs" (Stegocephali, Stereospondyli) from Madagascar, with remarks on their comparative ontogeny. J Vert Paleontol 23:544–555.

Steyer JS, Laurin M, Castanet J, Ricqlès de A. 2004. First histological and skeletochronological data on temnospondyl growth: palaeoecological and palaeoclimatological implications. Palaeogeogr Palaeoclimatol Palaeoecol 206:193–201.

Straehl FR, Scheyer TM, Forasiepi AM, MacPhee RD, Sánchez-Villagra MR. 2013. Evolutionary patterns of bone histology and bone compactness in xenarthran mammal long bones. PloS One 8: e69275.

Warren AA. 2000. Secondary aquatic temnospondyls of the Upper Permian and Mesozoic: the stereospondyls. In: Amphibian biology, Vol. 4, Paleontology: the evolutionary history of amphibians. Chipping Norton: Surrey Beatty and Sons. p 1123–1149.

Warren AA, Damiani R, Yates AM. 2006. The South African stereospondyl *Lydekkerina huxleyi* (Tetrapoda, Temnospondyli) from the Lower Triassic of Australia. Geol Mag 143:877–886.

Warren AA, Snell N. 1991. The postcranial skeleton of Mesozoic temnospondyl amphibians: a review. Alcheringa 15:43–64.

Watson DMS. 1920. The structure, evolution and origin of the Amphibia. The "orders" Rachitomi and Stereospondyli. Phil Trans R Soc B 209:1–73.

Witzmann F, Soler-Gijón R. 2010. The bone histology of osteoderms in temnospondyl amphibians and in the chroniosuchian *Bystrowiella*. Acta Zool-Stockholm 91:96–114.

Yates AM, Warren AA. 2000. The phylogeny of the 'higher' temnospondyls (Vertebrata: Choanata) and its implications for the monophyly and origins of the Stereospondyli. Zool J Linn Soc 128: 77–121.